The effect of pore size in an ultrasensitive DNA sandwich-hybridization assay for the *Escherichia coli* O157:H7 gene based on the use of a nanoporous alumina membrane

- Weiwei Ye[1,2], Tian Chen[2], Yijie Mao[2], Feng Tian[3], Peilong Sun[2] & Mo Yang[3]

Abstract

The authors describe a rapid method for the detection of the *Escherichia coli* O157:H7 (*E. coli* O157:H7) bacterial gene. The DNA sandwich-hybridization impedimetric assay is based on the use of a nanoporous alumina membrane in combination with gold/silver core/shell nanoparticles (Ag@AuNPs) that act as tags for impedance signal amplification. The probe oligonucleotides were immobilized on the walls of the nanopores. This is followed by hybridization, first with target (analyte), then with reporter oligonucleotides labeled with Ag@AuNP tags. The impedimetric signal results from target oligo hybridization with probe oligos and co-hybridization with labeled reporter oligos, which increases the blocking degree of the nanopores. The assays were tested with membranes in nanopore sizes of 20 nm, 50 nm and 100 nm. The assay performs best in case of 100 nm nanopores where the limit of detection is as low as 11 pM, with a linear detection range that extends from 50 pM to 200 nM. This indicates its potential for rapid and ultrasensitive gene detection.

Introduction

One of the major foodborne and water-borne pathogens, *Escherichia coli* O157:H7 (*E. coli* O157:H7) can produce toxins with great virulence and pathogenicity that cause gastrointestinal discomfort and even kidney failure [1, 2]. The foodborne diseases caused by *E. coli* O157:H7 are increasingly to be a serious threat to people's health and lead to million-dollar losses. Data from the Centers for Disease Control and Prevention Estimation showed that the harmful foodborne pathogens infected an estimated 265,000 people in the U.S. each year. Therefore, efficient and fast recognition of *E. coli* O157:H7 is essential for prevention of foodborne disease outbreak.

The most traditional microbiological methods, such as plate counting, multiple-tube fermentation and colony culture are used for sensitive foodborne pathogen detection [3, 4]. These methods are time-consuming and labor-intensive. They need complicated preparation procedures and 24 to 48 h incubation before suspected pathogens are detected. Enzyme-linked immunosorbent assay (ELISA) can overcome the shortcomings and has advantages of rapidness and reliability, but it is high-cost [5]. Polymerase chain reaction (PCR) for bacteria gene detection has rather good specificity and sensitivity. However, it bears limitation of expensive and sophisticated equipment and the need for skilled laboratory personnel with complicated experimental procedures [6, 7]. Thus, an inexpensive and convenient biosensor is needed for rapid detection of pathogenic *E. coli* O157:H7.

Biosensors have become promising means for detecting foodborne pathogens rapidly and sensitively [8,9,10]. Nucleic acid biosensors, which are based on DNA hybridization between probe oligonucleotides and target bacterial oligonucleotides, have been developed for foodborne pathogen identification. According to different detection mechanisms, there are quartz crystal microbalance (QCM) biosensors, surface plasmon resonance (SPR) biosensors, optical biosensors and electrochemical biosensors [11,12,13,14,15]. Nanomaterial-based DNA biosensors are good options for bacteria gene detection with the advantages of convenient reproduction, enhanced sensitivity, and selectivity [16, 17].

Nanoporous membranes, one kind of the various nanomaterials, have attracted much interest in biosensing. They are fabricated with a standard process and low-cost. Their high surface-to-volume ratio allows a large number of target molecules to be captured on the nanopore walls [18]. Nanoporous membrane based electrochemical biosensors are applied for detecting proteins, histamine and bacteria high sensitively [19,20,21,22]. Nanoporous membrane based impedance sensors have also been used for nucleic acid detection, analysis and sequencing [23, 24]. During the nucleic acid detection process, target oligos were captured by probe oligos covalently linked on nanopore walls and blocked part of the nanopores. The sensing mechanism is based on monitoring impedance increase due to the ion current blockage through the nanopores. Wang et al. developed a nanoporous membrane based impedance assay to detect *E. coli* O157:H7 gene [25]. However, it was developed and used for double-strand probe oligo and target oligo hybridization on nanopore walls. It does not fully block the ion current through the nanopores. In order to increase the blocking effect and detection sensitivity, one possible way is to label target DNA with tags. The tags can add additional blocking effect inside the nanopores and enhance the impedance signals of DNA hybridization [26]. In the field detection, labeling target oligos with nanoparticle tags made this method not applicable for biosensing applications.

In the study, nanoporous alumina membrane based DNA sandwich-hybridization structure impedance assays were developed for ultrasensitive *E. coli* O157:H7 gene detection with gold/silver core/shell on gold nanoparticle cores (Ag@AuNP) tags for impedimetric signal amplification. In this DNA sandwich-hybridization assay, probe oligos were firstly immobilized on nanopore walls. Target bacteria oligos hybridized with the probe oligos and reporter oligos which were labeled with Ag@AuNP tags. The hybridization of nanoparticles labeled reporter oligos with target bacteria oligos can increase the pore blocking degrees, leading to increased detection sensitivity. This nanoporous membrane combined with Ag@AuNP tags for DNA sandwich-hybridization structure assay of bacterium gene allowed sensitive target gene detection without target labeling. Nanoporous membranes with various nanopore sizes were investigated for this approach. The 100 nm nanopores achieved the lowest limit of detection (LOD) of 11 pM for *E. coli* O157:H7 bacterium gene detection.

Experimental

Materials

Sodium citrate, gold (III) chloride hydrate ($HAuCl_4 \cdot 3H_2O$), DL-Dithiothreitol (DTT), phosphate buffered saline (PBS), gold nanoparticles (AuNPs, 30 nm) and silver enhancer kit including solution A (silver salt), solution B (initiator), and sodium thiosulfate were purchased from Sigma Aldrich (St. Louis, Missouri, USA, www.sigmaaldrich.com). Desalting column (illustra MicroSpin G-25) was bought from GE Healthcare (Piscataway, NJ, USA, www.gelifesciences.com). Sylgard 184 silicone elastomer was bought from Dow Corning (Midland, Michigan, USA, www.dowcorning.com). A gene fragment (50 bases) of *E. coli* O157:H7 intimin (eaeA) gene (GenBank: U32312.1) with the sequence of 5′-TTTCAGGGAATAACATTGCTGCAGGATGGGCAACTCTTGAGCTTCTGTA A-3′ was used as the target gene. Amino modified probe oligo (5′−/5AmMC6/TTACAGAAGCTCAAGAGTTGCCCAT-3′), six bases mismatch gene fragment (5′-TTTCAGCGAATAACAATGCTGCACGATGGGCATCTCTTGTGCTTCTGTT A-3′), noncomplementary gene segment (5′-CCCAGAAAGGATGACGGATCAAGTATCATTACCTGTGGTCTTGGTGAC CC-3′), and thiol modified reporter oligo (5′-CCTGCAGCAATGTTA TTCCCTGAAA/3ThioMC3-D/−3′) were synthesized and provided by Integrated DNA Technologies (IDT, Voralville, IA, USA, www.idtdna.com).

Nanoporous membrane functionalization

The surface modification scheme for nanoporous membrane is shown in Fig. S1. Nanoporous membranes were immersed in boiled hydrogen peroxide (H_2O_2) for 30 min to form hydroxyl groups on membrane surfaces and nanopore walls. Then, the membranes were rinsed in DI water and dried. They were transferred into the mixture of toluene and GPMS (2%) at the temperature of 60 °C and stayed for about 20 h, followed by washing thoroughly using toluene and anhydrous ethanol successively. They were cured at 60 °C for 2 h to form epoxy groups on the membrane surfaces [27]. Probe oligos in PBS solution (pH 8.4) were then incubated with functionalized nanoporous alumina membranes for 2 h to be immobilized on membrane surfaces by covalent bonding.

Preparation of AuNPs

AuNPs were synthesized using a citrate synthesis approach with chloroauric acid ($HAuCl_4$) as the starting material [28]. Briefly, a beaker was washed with aqua regia and pure water before synthesis. DI water (20 mL) was added into the beaker and heated to boiling on a stirring hot plate with a magnetic stir bar. $HAuCl_4$ (1.0 mM, 6 μL) was quickly dropped to the boiling water with stirring. Sodium citrate solution (1%, 2 mL) was then mixed with the above solution rapidly. When the solution color turned

deep red, heating was turned off while the stirring was not turned off until the temperature decreased to room temperature.

AuNP-reporter oligo conjugation

Thiol modified reporter oligonucleotides were firstly activated by DTT and purified by passing the desalting column. The activated monothiolated reporter oligos were then added to AuNPs solution immediately and vortexed. The mixture stayed for 12 h at room temperature and was aged with sodium solution. In 16 h, the mixture was centrifuged at 12,000 r/min for 40 min. The supernatant including unreacted oligonucleotides was removed and the left AuNP-reporter oligo conjugation was redispersed in PBS solution. By repeating the above processes for 3 times, the washed AuNP-reporter oligo conjugation was dispersed in PBS (pH 7.4) and characterized by UV-Vis absorption spectra.

Ag@AuNP tags formation

AuNP-reporter oligo conjugation hybridized with target oligos, which were captured by probe oligos on nanoporous membrane. Ag@AuNP tags were formed by the process of silver enhancement on AuNPs using silver enhancer kit. The reaction principle is shown in Eq. 1. AuNPs have catalytical properties and can catalyze silver metal deposition on their surfaces with silver ions and a reducing agent hydroquinone in solution.

volume of solution A and solution B from silver enhancer kit was mixed and immediately added to AuNPs. In 5 min, a thin metal silver layer was formed on AuNPs surfaces to form Ag@AuNP tags via reduction from silver ions. Sodium thiosulfate (2.5%) was used to fix the silver on AuNPs for 2–3 min.

Characterization

The size and morphology of AuNPs and Ag@AuNP tags were observed by a transmission electron microscopy (TEM, JEOL-2100F, Japan). Nanoporous alumina membranes were characterized by scanning electron microscopy (SEM, JSM-6490, Japan). Zeta potential and hydrodynamic diameter were measured by a Zetasizer Zeta Potential Analyzer (Malvern Instruments Ltd., England). Fluorescence images were obtained from a fluorescence microscope (Nikon Eclipse 80i, Nikon, Japan). X-ray photoelectron spectroscopy (XPS) analysis was taken by the system of electron spectrometer (Sengyang SKL-12) equipped with a VG CLAM 4MCD electron energy analyzer. Al Kα source (1253.6 eV) operated with an accelerating voltage of 10 kV and emission current of 15 mA.

Electrochemical impedance spectroscopy measurement

A testing PDMS chamber, which consisted of an upper section and a bottom section with different diameters, was made from Sylgard 184 silicone elastomer via thermal curing. The modified nanoporous membranes were anchored in the edge of PDMS chamber between the upper and the bottom sections. Electrochemical impedance spectroscopy was recorded via a two-electrode system with two platinum wire electrodes put in the bottom chamber and upper chamber. The impedance measurement was performed on an electrochemical analyzer VersaSTAT3 (METEK) with 50 mVpp voltage at room temperature. The impedance signal changes of probe oligo immobilization, target oligo hybridization, co-hybridization with reporter oligos with Ag@AuNP tags were recorded.

Results and discussion

Mechanism of sandwich-structure assay

The detection mechanism for *E. coli* O157:H7 bacterium gene sensing by the platform of nanoporous membrane based DNA sandwich-hybridization structure assay is shown in Fig. 1. Two platinum wire electrodes were placed across the nanoporous alumina membrane (Fig. 1a). The performances of probe oligo immobilization, target oligo detection, and hybridization with reporter oligos with or without Ag@AuNP tags in the nanopores were investigated by impedance spectra. Nanoporous alumina membranes with various nanopore sizes were applied as core chips for constructing biosensors. The detailed processes of DNA detection in nanopores causing nanopore blockage are shown in Fig. 1b, c and d. Membranes with 20 nm nanopores were appropriate for oligo detection without Ag@AuNP tags because the nanopores were not large enough for AuNPs entering. For nanoporous membranes immobilized with probe oligos, electrolyte ions flow through nanopores freely and the current was relatively large (Fig. 1b_1). The hybridization of target bacteria oligos with probe oligos brought the blocking effect in the nanopores and decreased the ion flow. It led to the decrease of electrolyte current and increase of impedance signals (Fig. 1b_2). Membranes with 50 nm and 100 nm nanopores were applicable for oligo detection with Ag@AuNP tags. The immobilization of probe oligos and hybridization with target oligos blocked the nanopores and increased the impedance (Fig. 1c_1, c_2 and d_1, d_2). The target bacteria oligos co-hybridized with reporter oligos with Ag@AuNP tags. The blocking effect for ion flow was increased significantly and impedance signals were amplified (Fig. 1c_3, d_3). By recording impedance signals and calculating the signal changes across the nanoporous alumina membranes, the *E. coli* O157:H7 bacterium gene can be detected.

Fig. 1

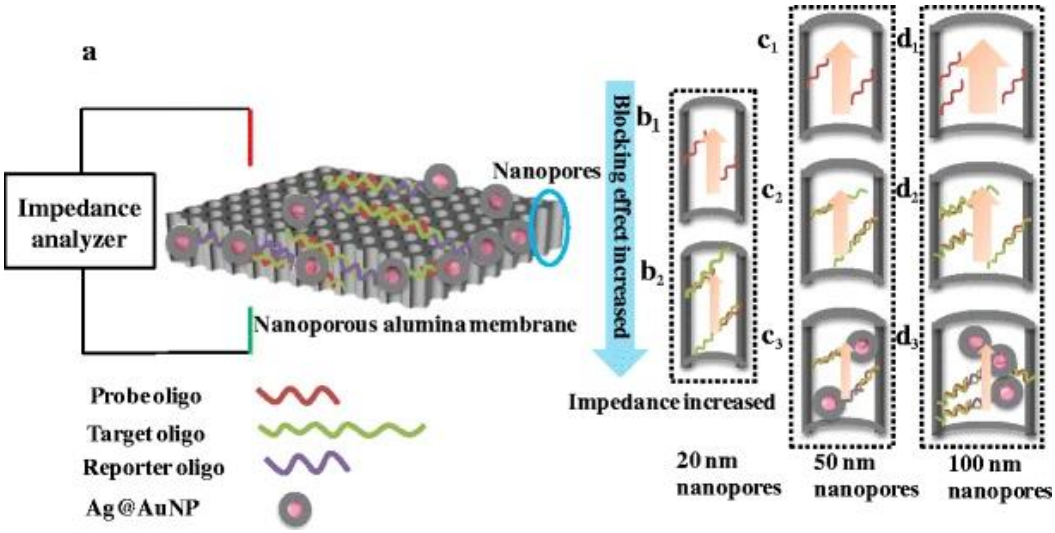

The sensing mechanism of the DNA sandwich-hybridization structure assay biosensor for *E. coli* O157:H7 bacterium gene detection

Choice of materials

Metal nanoparticles, such as AuNPs and silver nanoparticles (AgNPs), have extraordinary size-dependent optical properties and high surface area to volume ratio that have been extensively used as labels for various biomedical applications [29]. The sensing mechanism of this study is based on nanopore blocking induced impedance sensing. AuNPs and AgNPs are often used as tags for increasing blocking effect. However, when the nanoparticles have large matching size to nanopores, it is difficult to go inside due to the hydrodynamic interaction between nanopore wall and nanoparticles. When the size of nanoparticles is smaller than nanopore size, it is easy for nanoparticles to enter the nanopores but they cannot block the nanopores efficiently. So both AuNPs and AgNPs labeling cannot achieve easy entering the nanopore and large blocking effect at the same time. To solve this problem, we developed an approach to let seed AuNP with reporter oligos enter the nanopore and hybridize with oligos on the nanopore wall. AuNPs can catalyze silver ion to deposit silver shell on AuNPs surfaces to form larger size Ag@AuNP tags inside the nanopore wall, which can achieve both easy entering and large blocking of the nanopores with increased impedance signals. So in the study, we used Ag@AuNP tags for nanopore blocking induced impedance sensing.

Characterization of nanoparticles and target DNA capture inside nanopores

The AuNP-reporter oligo conjugation was characterized by TEM as shown in Fig. 2a. The AuNP-reporter oligo is well-distributed and had good stability in solution. The average diameter of the AuNPs is 15 nm. A thin oligo layer was observed around AuNPs surface with the thickness of 1 nm. The HRTEM image (Fig. 2b) shows the fringe spacing to be 2.35 Å, having good match with the d-spacing of (111) plane gold crystal structure. The selected area electron diffraction pattern (SAED) (Fig. 2b inset)

indicates the good crystallinity of an entire nanoparticle [30]. UV absorbance and zeta potential were further used to characterize the AuNPs and AuNP-reporter oligo conjugation. The main UV absorption peak of AuNPs was at 520 nm. Fig. S2a shows the UV absorbance of AuNPs and AuNP-reporter oligo conjugation. The absorption peak shifted from 520 nm to 524 nm after oligo conjugation. Zeta potential measurement results showed that the average potential of AuNPs shifted from −49.77 mV to −20.89 mV after AuNPs conjugated with oligos (Fig. S2b). The less negatively charged AuNP-reporter oligo conjugation was mainly due to the charges of conjugated oligonucleotides. The hydrodynamic diameters of AuNPs and AuNPs-oligo conjugation were 26.4 nm and 53.1 nm, respectively. Therefore, UV absorbance, zeta potential and hydrodynamic diameter results supported the TEM observation. Silver was deposited on AuNPs to form Ag@AuNPs that were characterized by TEM (Fig. S2c). The average diameter of Ag@AuNPs was about 30 nm. The volume was eight times that of 15 nm AuNPs. Energy spectrum analysis is shown in Fig. S2d. The presence of Au and Ag components demonstrated the successful deposition of Ag shell on AuNPs.

Fig. 2

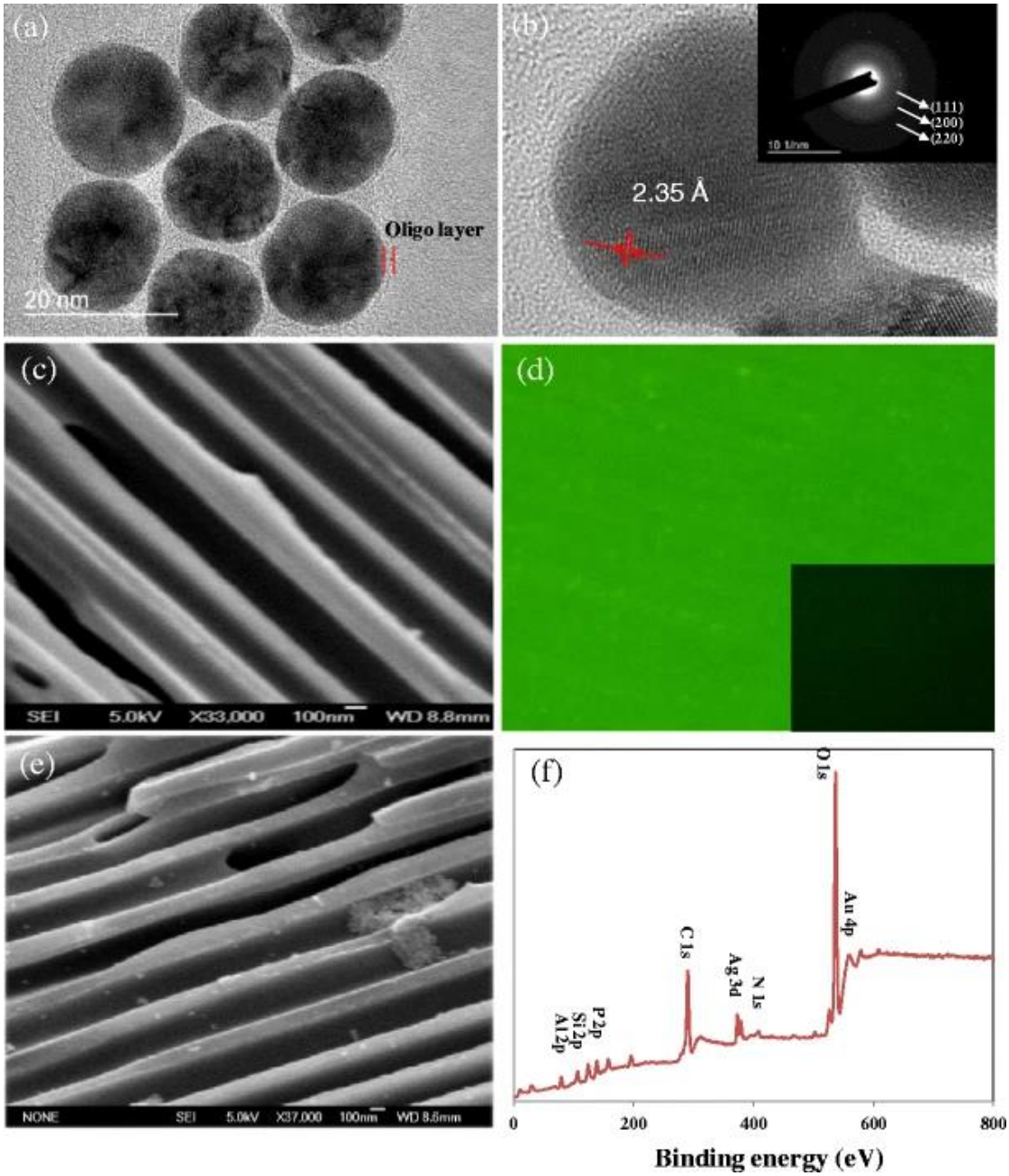

a TEM image of AuNP-oligo conjugation dispersed in DI water; (**b**) HRTEM image of a single AuNP and SAED pattern (inset). **c** SEM image of cross-sectional view of nanoporous alumina membrane without surface modification; (**d**) fluorescence images of functionalized nanoporous membrane after capturing fluorescein-labeled target *E. coli* O157:H7 gene oligos; dark image of the probe oligos immobilized nanoporous alumina membrane (inset); (**e**) SEM image of oligo hybridization with Ag@AuNP tags on nanoporous alumina membrane; (**f**) XPS wide scan of nanoporous alumina membranes after oligo hybridization with Ag@AuNP tags

The cross-sectional view of nanoporous membrane without surface modification was observed by SEM image with the result shown in Fig. 2c. It was found that there was nothing blocking in the nanopores. Fluorescein-labeled target oligonucleotides captured by probe oligos immobilized on the nanoporous membrane displayed green

emission (Fig. 2d). In comparison with the dark image of the probe oligos immobilized nanoporous alumina membrane (inset image in Fig. 2d) under fluorescence microscopy, the fluorescence signals demonstrated the successful detection of target bacteria *E. coli* O157:H7 gene oligos. SEM was used to characterize the hybridization of target oligos with probe oligos and reporter oligos with tags in the nanopores (Fig. 2e). It is observed that clusters of Ag@AuNP tags were attached on nanopore walls. It showed that target *E. coli* O157:H7 bacterium gene oligos were specifically detected by hybridization with probe oligos. Figure 2f presents the XPS wide scan of nanoporous membrane with complementary oligo hybridization with Ag@AuNP tags. The principle elements, including Au, Ag, Al and N, were present in the spectrum. This demonstrated the hybrid combination of complementary oligo hybridization on nanoporous alumina membrane and successful attachment of nanoparticle tags.

Impedance spectroscopy detection

The nanoporous membrane based DNA sandwich-hybridization structure biosensor with Ag@AuNP tags was used to investigate target oligo detection of *E. coli* O157:H7 bacterium gene via electrochemical impedance spectroscopy. Probe oligos with different concentrations were immobilized on nanoporous alumina membranes with 20 nm, 50 nm and 100 nm nanopores. Impedance increased with increasing probe oligo concentrations. The impedance amplitude reached maximum at the concentrations of 0.5 μM, 0.4 μM, 0.2 μM for 20 nm nanopores (Fig. S3), 50 nm nanopores (Fig. S4) and 100 nm nanopores (Fig. S5), respectively. Therefore, nanoporous membranes with 20 nm nanopores capture the largest amount of oligos, which is explained by the nanoporous membrane area factor α described in Eq. 2.

Where d and l are the diameter and the length of nanopore, respectively. Small diameters and long nanopores make large surface areas. Membranes with 20 nm nanopores have the largest surface area for probe oligos immobilization. With the same nanopore length, surface area decreases for 50 nm nanopores and 100 nm nanopores. Therefore, the amount of captured oligos decreased.

Figure 3a shows impedance spectra of probe oligo immobilization and hybridization with target oligos in the 20 nm nanopores. Impedance increased with 0.5 μM probe oligos immobilization and hybridization with 0.5 μM target oligos on nanoporous membrane. Figure 3b shows impedance amplitude changes with various target oligo concentrations. The impedance amplitude increased linearly. The linear equation was $y = 16.216\times-0.6332$ with $R^2 = 0.99$ and the LOD was calculated about 95 nM.

Fig. 3

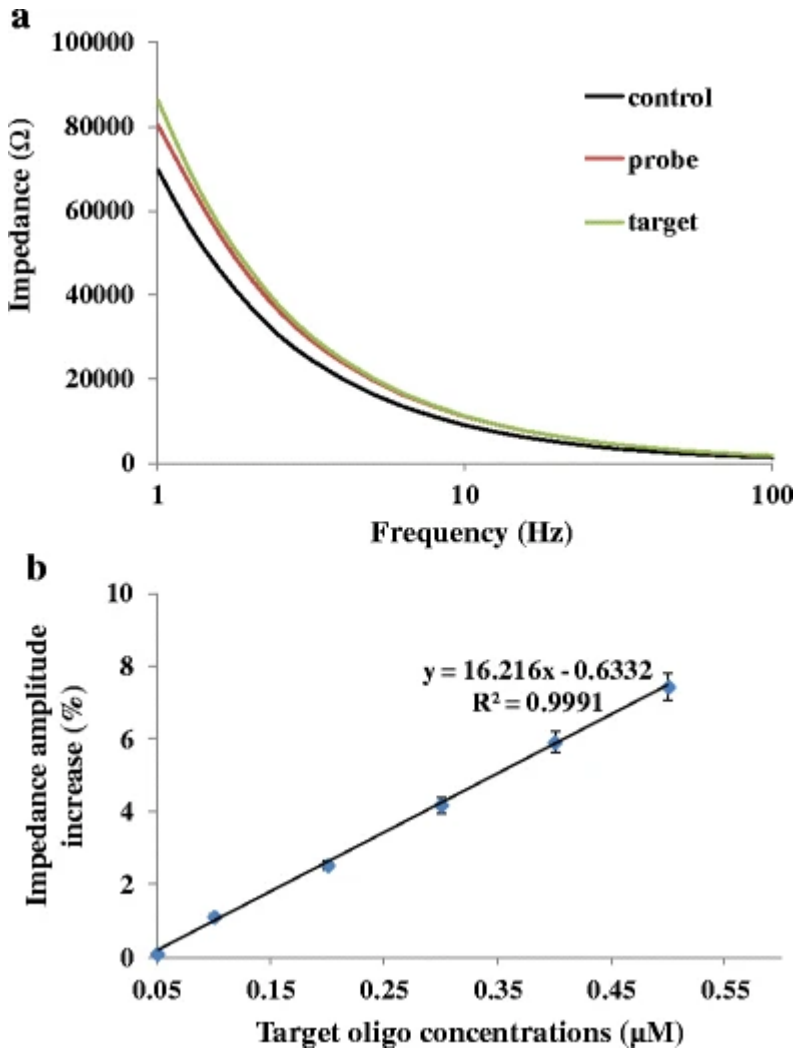

a Impedance spectra of probe oligo immobilization and target oligo detection on nanoporous alumina membrane with 20 nm nanopores; (**b**) impedance amplitude changes of different target oligo concentrations

Nanoporous membranes with 50 nm nanopores were applied for constructing electrochemical biosensors with Ag@AuNP tags for DNA sandwich-hybridization structure assay of *E. coli* O157:H7 bacterium gene. Probe oligos were immobilized in nanopores, and target oligos were detected and hybridized with probe oligos. The reporter oligos with Ag@AuNP tags were hybridized with target oligos. These four processes were analyzed by impedance spectra in Fig. 4a. Impedance increased with probe oligo immobilization, target oligo hybridization, and co-hybridization with reporter oligos with Ag@AuNP tags. The amplitude increased linearly with the equation for target oligo detection without tags $y = 12.048\times + 2.6051$ with $R^2 = 0.98$, with Ag@AuNP tags $y = 79.517\times + 7.3922$ with $R^2 = 0.98$, respectively (Fig. 4b). The gradient of linear curve increased with Ag@AuNP tags showing the rise of detection sensitivity. Figure 4c shows impedance amplitude changes for target oligo detection without tags and Ag@AuNP tags for low target oligo concentrations ranging from 1 nM to 200 nM. Impedance amplitude increased much more with Ag@AuNP tags than that without tags. The LOD was calculated about 7 nM.

Fig. 4

a Impedance spectra of probe oligo immobilization, target oligo detection with and without Ag@AuNP tags on nanoporous alumina membrane with 50 nm nanopores; (**b**) impedance amplitude change of different target oligo concentrations with and without Ag@AuNP tags. **c** impedance amplitude change of low target oligo concentrations with and without Ag@AuNP tags

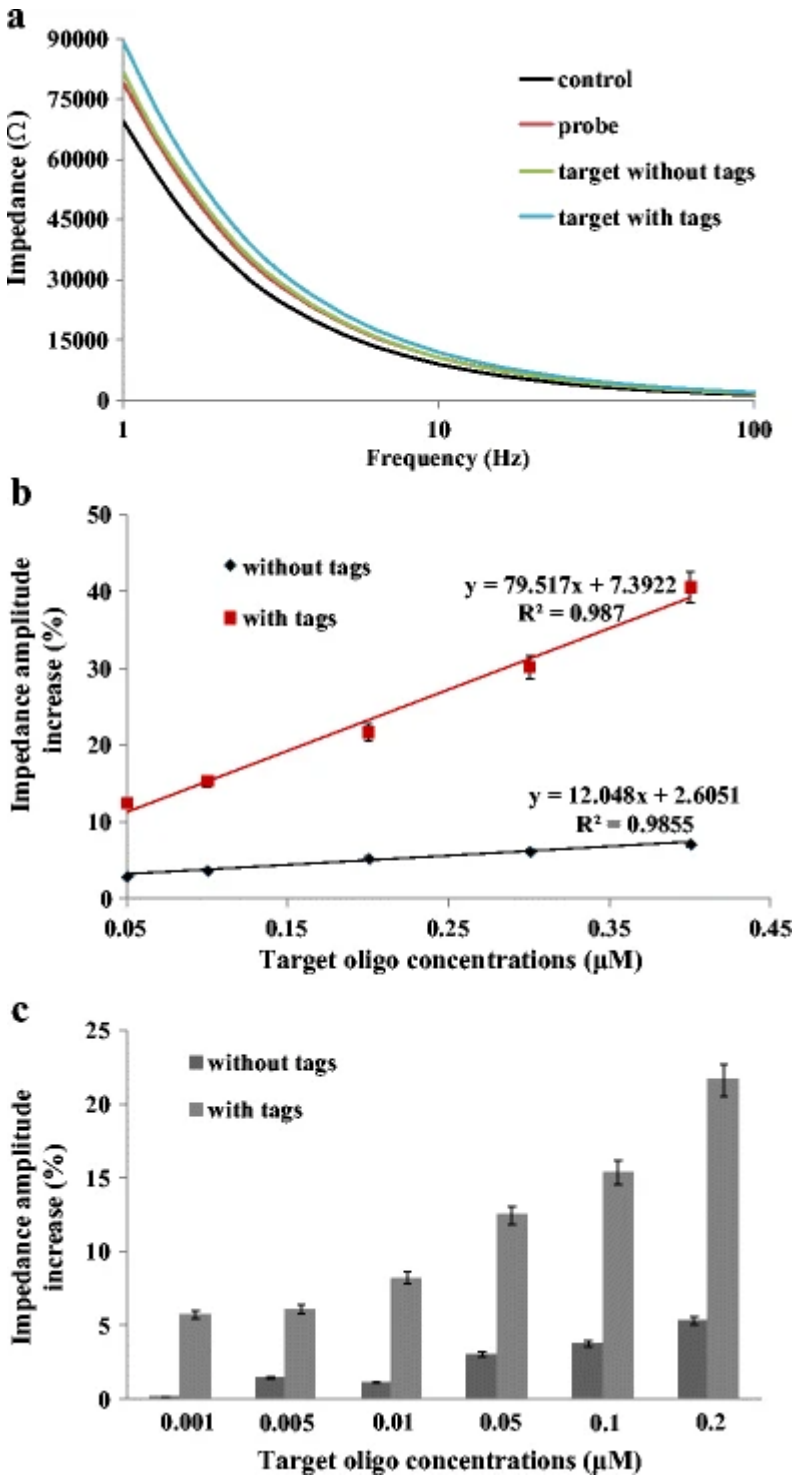

E. coli O157:H7 bacterium gene detection by nanoporous alumina membranes with 100 nm nanopores was studied. Figure 5a shows impedance spectra across nanoporous alumina membrane for target oligo detection without and with Ag@AuNP tags. Impedance amplitude increased after immobilization of probe oligos, hybridization with target oligos, co-hybridization with reporter oligos with Ag@AuNP tags. Ag@AuNP tags amplified the impedance amplitude increase, which became large obviously. The impedance amplitude and the logarithm of target oligo concentrations

had linear correlation (Fig. 5b). The correlation for target oligo of *E. coli* O157:H7 gene detection without tags is presented by equation $y = 1.2219\ln(x) + 4.3541$, with $R^2 = 0.96$. The equation for target gene oligo detection with Ag@AuNP tags is $y = 2.9976\ln(x) + 15.317$ with $R^2 = 0.98$. The slope increase of correlation curves demonstrated the improvement of detection sensitivity with Ag@AuNP tags. In order to compare the impedance enhancement of Ag@AuNP tags and AuNPs with the identical size, AuNPs with the diameter of 30 nm were used as tags for 20 nM target oligo detection. The impedance increased about 7.9% with AuNPs. The calculated impedance amplitude increase with Ag@AuNP tags was about 24%. The impedance amplitude increase with AuNPs was much less than that with Ag@AuNP tags because large AuNPs cannot enter nanopores efficiently. Figure 5c shows the relative impedance amplitude change for assays based on nanoporous membrane with and without Ag@AuNP tags to investigate amplification effect at low concentrations for target oligo detection. It indicated that impedance amplitude enhancement with Ag@AuNP tags became obvious as the concentrations of target oligos increased in the range of low concentrations. The LOD was calculated as low as 11 pM. This nanoporous alumina membrane based sandwich structure assay for *E. coli* O157:H7 bacterium gene detection had high sensitivity and low LOD, which showed the potential for on-site bacteria gene detection.

Fig. 5

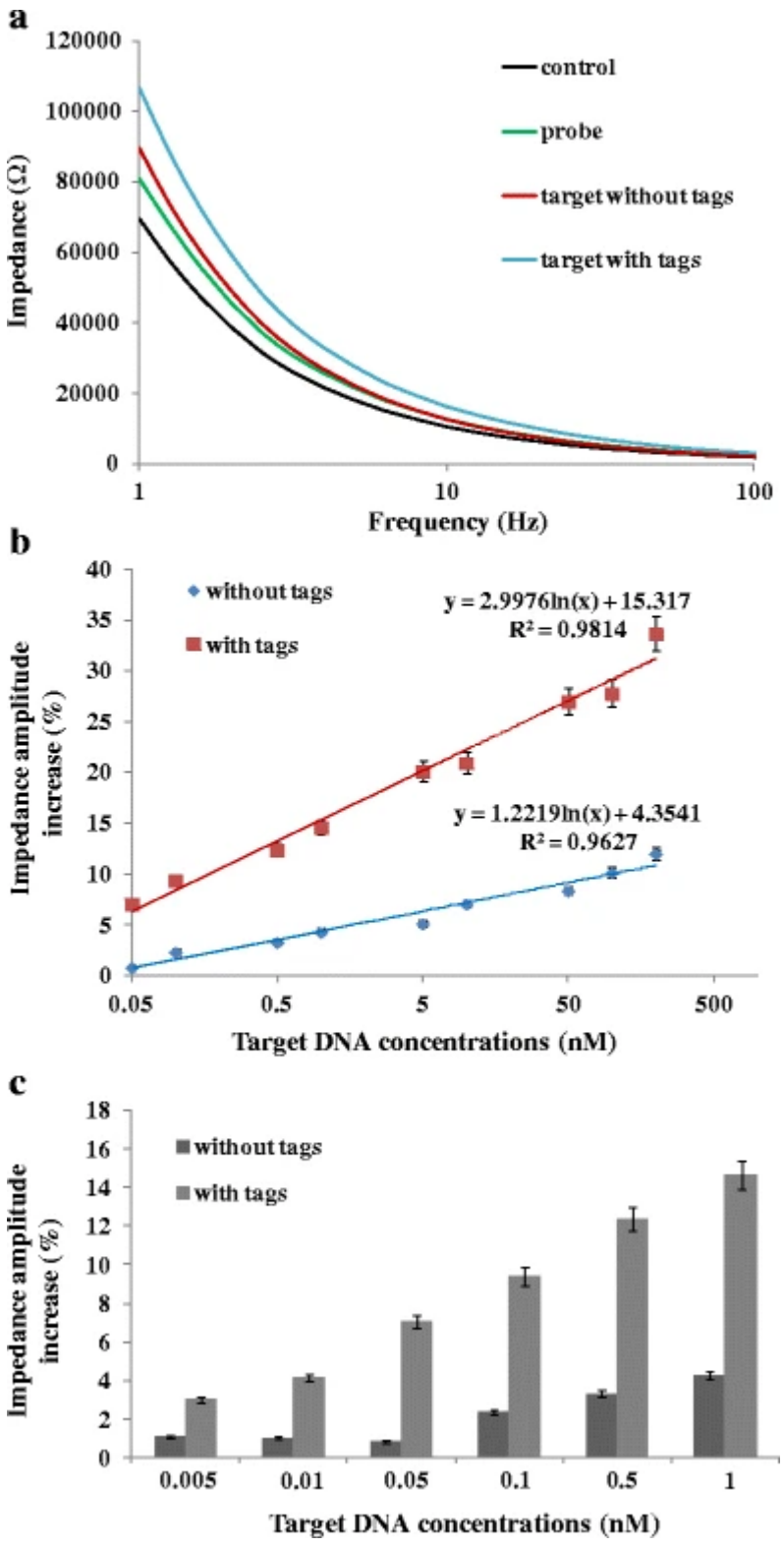

a Impedance spectra of probe oligo immobilization, target oligo detection with and without Ag@AuNP tags on nanoporous alumina membrane with 100 nm nanopores; (**b**) impedance amplitude change of different target oligo concentrations with and without Ag@AuNP tags. **c** impedance amplitude change of low target oligo concentrations with and without Ag@AuNP tags

With the through nanopores and large surface areas, nanoporous alumina membranes were good choices for constructing impedance biosensors. Compared to 20 nm nanopores, membranes with 50 nm and 100 nm nanopores facilitated nanoparticle tags for impedance signal amplification, resulting in increased detection sensitivity and low LOD. Although membranes with 50 nm nanopores had higher surface area than membranes with 100 nm nanopores, membranes with 100 nm nanopores obtained higher detection sensitivity and lower LOD. It may be due to the good efficiency of nanoparticles entering 100 nm nanopores. Nanoporous membranes with 100 nm nanopores presented the potential application in sandwich structure assay of bacteria gene.

Specificity of sandwich-structure assay

To investigate the detection specificity of DNA sandwich-hybridization structure assay based on nanoporous membranes, 6 bases mismatch and non-complementary oligonucleotides with the concentration of 200 nM were detected. In nanoporous alumina membranes with 50 nm nanopores, impedance increased significantly for target oligo detection compared to impedance spectrum of probe oligo immobilization. But it showed no significant increase with 6 bases mismatch oligos and noncomplementary oligos (Fig. 6a). Figure 6b shows impedance amplitude change of target oligo, 6 bases mismatch oligo and noncomplementary oligo detection in comparison with probe oligo immobilization. Impedance amplitude increased about 23.5% for target oligo detection of *E. coli*O157:H7 bacterium gene. However, it increased only about 3.8% and 3% for 6 bases mismatch and non-complementary oligo detection, which showed the good specificity of the sensing platform.

Fig. 6

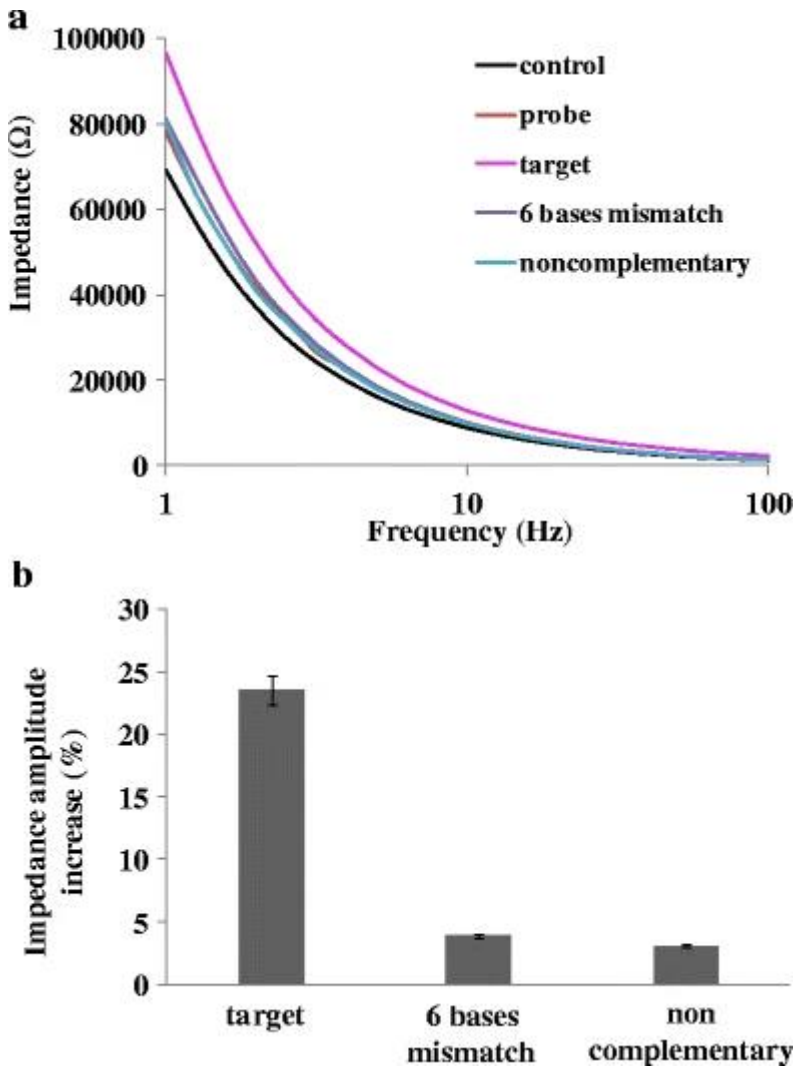

a Impedance spectra and (**b**) impedance amplitude change of probe oligo immobilization, target oligo hybridization detection, 6 bases mismatch oligo and noncomplementary oligo detection on nanoporous alumina membranes with 50 nm nanopores

The specificity of DNA sandwich-hybridization structure assay for oligo detection based on nanoporous alumina membranes with 100 nm nanopores was investigated as well. Impedance spectrum for 100 nM target oligo detection had great differentiation from the spectra of probe oligo. The impedance spectrum for the same concentration of 6 bases mismatch oligo and noncomplementary oligo detection had little differentiation (Fig. 7a). The impedance amplitude increased about 26.4%, 3.6% and 1.7% for target oligos of *E. coli* O157:H7 bacterium gene hybridization assay, 6 bases mismatch and non-complementary oligo detection (Fig. 7b). This nanoporous alumina membrane with 100 nm nanopores based sensing platform showed good specificity for specific *E. coli*O157:H7 gene sequence detection.

Fig. 7

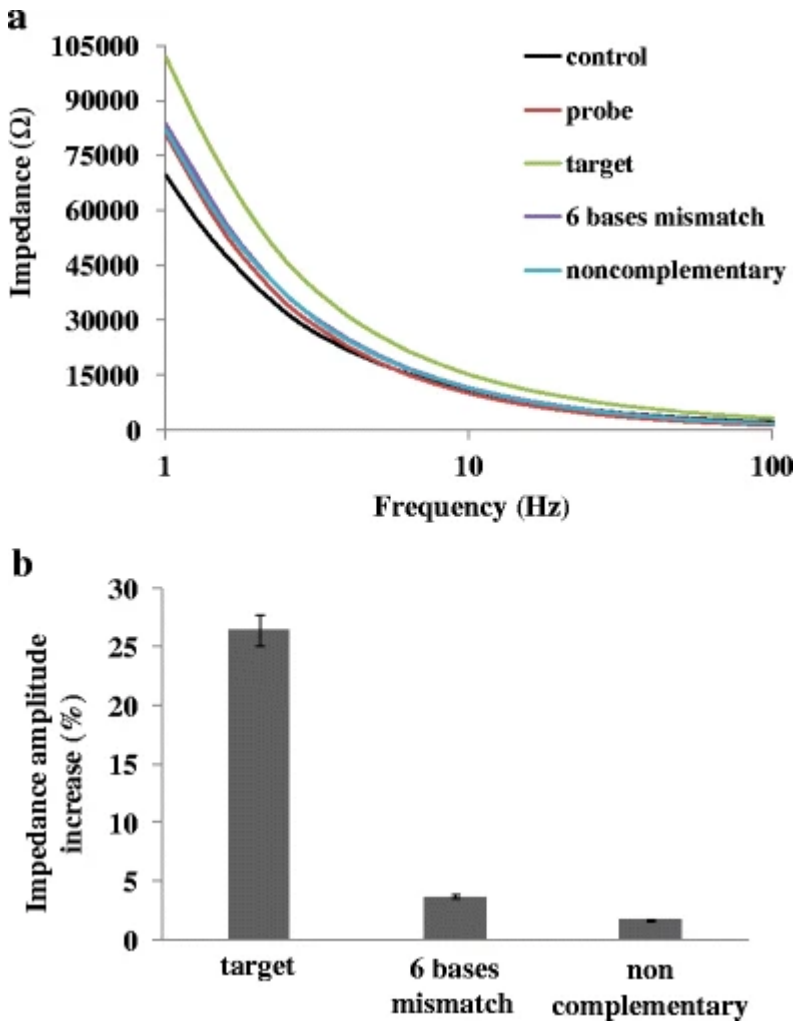

a Impedance spectra and (**b**) impedance amplitude change of target oligo capture and hybridization, 6 bases mismatch oligo and noncomplementary oligo detection on nanoporous membranes with nanopore diameter of 100 nm

DNA sandwich-hybridization structure assay based on membranes with both 50 nm nanopores and 100 nm nanopores with Ag@AuNP tags had excellent specificity for *E. coli* O157:H7 bacterium gene detection. Nanoporous alumina membranes with 20 nm nanopores were used for constructing impedance biosensors for *E. coli* O157:H7 bacterium gene detection without nanoparticle tags. The 50 nm nanopores and 100 nm nanopores showed the potential for establishing DNA sandwich-hybridization structure assay for *E. coli* O157:H7 bacterium gene detection with great sensitivity. Membranes with 100 nm nanopores allowed nanoparticles to enter the nanopores efficiently, which made them achieve the best detection sensitivity and lowest LOD for bacteria gene detection. The analytical performance of the DNA sandwich-hybridization structure assay based on membranes with Ag@AuNP tags is compared with that of some reported methods in Table 1. It shows a comparative study on *E. coli* detection by various methods and materials applied. Compared with these reported methods, such as immunoassay, ELISA and QCM for *E. coli* bacteria detection, our method presented

here detects bacteria gene with the advantages in its low cost, excellent sensitivity, specificity and low LOD.

Table 1 An overview on the reported nanomaterial-based methods for determination of *E. coli*

Materials used	Method applied	LOD	Specificity	References
Magnetic microbeads	Fluorescence	50 CFU/mL	Highly Selective	[31]
Gold nanofilm/Magnetic dynabeads	Giant magnetoimpedance (GMI) sensor	50 CFU/mL	Specific	[32]
AuNPs	Immunoassay	10^2 CFU/mL	Specific	[33]
Gold electrode	QCM	10^2 CFU/mL	High sensitivity	[34]
Beacon AuNPs	ELISA	10^3 CFU/mL	High specificity	[35]
Nanoporous alumina membrane/Ag@AuNP tags	Electrochemical biosensors	11 pM	Excellent specificity	This work

Conclusions

In this work, a DNA sandwich-hybridization impedance assay based on nanoporous alumina membrane has been developed for *E. coli* O157:H7 bacterium gene detection with Ag@AuNP tags. Ag@AuNP tags were used for labeling at the end of reporter oligos without the need of labeling target oligos. It is applicable in-field detection of *E. coli* O157:H7 bacterium gene. This assay was capable of detecting target oligos with high sensitivity and discriminating mismatched and noncomplementary oligos with excellent specificity on the nanoporous membrane platform. The detection sensitivity was affected by the nanopore sizes. With the advantages of multiple nanopore sizes, the nanoporous alumina membrane based DNA sandwich-structure impedance assay can be developed as a versatile tool for rapid foodborne pathogen analysis in bioanalytical and clinical diagnostic applications.

References

1. Steiner TS (2016) New insights into shiga toxigenic *Escherichia coli* pathogenesis: when less is more. J Infect Dis 213(8):1214–1215

   Article Google Scholar

2. Lewis SB, Cook V, Tighe R, Schüller S (2014) Enterohemorrhagic *Escherichia coli* colonization of human colonic epithelium *in vitro* and *ex vivo*. Infect Immun 83(3):942–949

   Article Google Scholar

3. Sun J, Ji J, Sun Y, Abdalhai MH, Zhang Y, Sun X (2015) DNA biosensor-based on fluorescence detection of *E. coli* O157:H7 by Au@Ag nanorods. Biosens Bioelectron 70:239–245

   CAS Article Google Scholar

4. Le Ru EC, Grand J, Sow I, Somerville WR, Etchegoin PG, Treguer-Delapierre M, Charron G, Félidj N, Lévi G, Aubard J (2011) A scheme for detecting every single target molecule with surface-enhanced raman spectroscopy. Nano Lett 11(11):5013–5019

   Article Google Scholar

5. Karmali MA (2004) Prospects for preventing serious systemic toxemic complications of Shiga toxin–producing *Escherichia coli* infections using Shiga toxin receptor analogues. J Infect Dis 189(3):355–359

   Article Google Scholar

6. Elizaquível P, Sánchez G, Aznar R (2012) Quantitative detection of viable foodborne *E. coli* O157:H7, *Listeria monocytogenes* and *Salmonella* in fresh-cut vegetables combining propidium monoazide and real-time PCR. Food Control 25(2):704–708

   Article Google Scholar

7. Desai PT, Walsh MK, Weimer BC (2008) Solid-phase capture of pathogenic bacteria by using gangliosides and detection with real-time PCR. Appl Environ Microbiol 74(7):2254–2258

   CAS Article Google Scholar

8. Ben Aissa A, Jara JJ, Sebastián RM, Vallribera A, Campoy S, Pividori MI (2017) Comparing nucleic acid lateral flow and electrochemical genosensing for the simultaneous detection of foodborne pathogens. Biosens Bioelectron 88:265–272

   CAS Article Google Scholar

9. Xu LZ, Lu Z, Cao LL, Pang HY, Zhang Q, Fu YC, Xiong YH, Li YY, Wang XY, Wang JP, Ying YB, Li YB (2017) In-field detection of multiple pathogenic bacteria in food products using a portable fluorescent biosensing system. Food Control 75:21–28
10. Pandey A, Gurbuz Y, Ozguz V, Niazi JH, Qureshi A (2017) Graphene-interfaced electrical biosensor for label-free and sensitive detection of foodborne pathogenic *E. coli* O157:H7. Biosens Bioelectron 91:225–231

    CAS Article Google Scholar

11. Mao XL, Yang LJ, Su XL, Li YB (2006) A nanoparticle amplification based quartz crystal microbalance DNA sensor for detection of *Escherichia coli* O157:H7. Biosens Bioelectron 21(7):1178–1185

12. Zhang D, Yan Y, Li Q, Yu T, Cheng W, Wang L, Ju H, Ding S (2012) Label-free and high-sensitive detection of *Salmonella* using a surface plasmon resonance DNA-based biosensor. J Biotechnol 160(3–4):123–128

CAS Article Google Scholar

13. Shi JY, Chan CY, Pang Y, Ye WW, Tian F, Lyu J, Zhang Y, Yang M (2015) A fluorescence resonance energy transfer (FRET) biosensor based on graphene quantum dots (GQDs) and gold nanoparticles (AuNPs) for the detection of mecA gene sequence of *Staphylococcus aureus*. Biosens Bioelectron 67:595–600

CAS Article Google Scholar

14. Ye WW, Tsang MK, Liu X, Yang M, Hao JH (2014) Upconversion luminescence resonance energy transfer (LRET)-based biosensor for rapid and ultrasensitive detection of avian influenza virus H7 subtype. Small 10(12):2390–2397

CAS Article Google Scholar

15. Zaino LP, Ma C, Bohn PW (2016) Nanopore-enabled electrode arrays and ensembles. Microchim Acta 183:1019–1032

CAS Article Google Scholar

16. Pérez-López B, Merkoç A (2011) Nanomaterials based biosensors for food analysis applications. Trends Food Sci Technol 22(11):625–639

Article Google Scholar

17. Savoye F, Feng P, Rozand C, Bouvier M, Gleizal A, Thevenot D (2011) Comparative evaluation of a phage protein ligand assay with real-time PCR and a reference method for the detection of *Escherichia coli* O157:H7 in raw ground beef and trimmings. J Food Prot 74(1):6–12

CAS Article Google Scholar

18. Tsang MK, Ye WW, Wang GJ, Li JM, Yang M, Hao JH (2016) Ultrasensitive detection of Ebola virus oligonucleotide based on upconversion nanoprobe/nanoporous membrane system. ACS Nano 10(1):598–605

CAS Article Google Scholar

19. Yu JJ, Liu ZB, Yang M, Mak A (2009) Nanoporous membrane-based cell chip for the study of anti-cancer drug effect of retinoic acid with impedance spectroscopy. Talanta 80(1):189–194
20. Ye WW, Xu YF, Zheng LH, Zhang Y, Yang M, Sun PL (2016) A nanoporous alumina membrane based electrochemical biosensor for histamine determination with fiofunctionalized magnetic nanoparticles concentration and signal Amplification. Sensors 16(10):1767–1778
21. Ye WW, Guo JB, Bao XF, Chen T, Weng WC, Chen S, Yang M (2017) Rapid and sensitive detection of bacteria response to antibiotics using nanoporous membrane and graphene quantum dot (GQDs)-based electrochemical biosensors. Materials 10(6):603–614

Article Google Scholar

22. Chan KY, Ye WW, Zhang Y, Xiao LD, Leung PHM, Li Y, Yang M (2013) Ultrasensitive detection of *E. coli* O157:H7 with biofunctional magnetic bead concentration via nanoporous membrane based electrochemical immunosensor. Biosens Bioelectron 41:532–537

CAS Article Google Scholar

23. Vlassiouk I, Takmakov P, Smirnov S (2005) Sensing DNA hybridization via ionic conductance through a nanoporous electrode. Langmuir 21(11):4776–4778

CAS Article Google Scholar

24. Shi J, Hou J, Fang Y (2016) Recent advances in nanopore-based nucleic acid analysis and sequencing. Microchim Acta 83:925–939

Article Google Scholar

25. Wang LJ, Liu QJ, Hu ZY, Zhang YF, Wu CS, Yang M, Wang P (2009) A novel electrochemical biosensor based on dynamic polymerase-extending hybridization for *E. coli* O157:H7 DNA detection. Talanta 78(3):647–652
26. Ye WW, Shi JY, Chan CY, Zhang Y, Yang M (2014) A nanoporous membrane based impedance sensing platform for DNA sensing with gold nanoparticle amplification. Sensors Actuators B Chem 193:877–882

CAS Article Google Scholar

27. Ye WW, Guo JB, Chen S, Yang M (2013) Nanoporous membrane based impedance sensors to detect the enzymatic activity of botulinum neurotoxin A. J Mater Chem B 1:6544–6550

CAS Article Google Scholar

28. Nguyen DT, Kim DJ, Kim KS (2011) Controlled synthesis and biomolecular probe application of gold nanoparticles. Micron 42:207–227

CAS Article Google Scholar

29. Yu L, Li N (2016) Binding strength of nucleobases and nucleosides on silver nanoparticles probed by a colorimetric method. Langmuir 32:5510–5518

CAS Article Google Scholar

30. Chen Y, Gu X, Nie CG, Jiang ZY, Xie ZX, Lin CJ (2005) Shape controlled growth of gold nanoparticles by a solution synthesis. Chem Commun 33:4181–4183

Article Google Scholar

31. Zeng Y, Wan Y, Zhang D (2016) Lysozyme as sensitive reporter for fluorometric and PCR based detection of *E. coli* and *S. aureus* using magnetic microbeads. Microchim Acta 183:741–748

CAS Article Google Scholar

32. Yang Z, Liu Y, Lei C, Sun XC, Zhou Y (2016) Ultrasensitive detection and quantification of *E. coli* O157:H7 using a giant magnetoimpedance sensor in an open-surface microfluidic cavity covered with an antibody-modified gold surface. Microchim Acta 183:1831–1837

CAS Article Google Scholar

33. Cui X, Huang YJ, Wang JY, Zhang L, Rong Y, Lai WH, Chen T (2015) A remarkable sensitivity enhancement in a gold nanoparticle-based lateral flow immunoassay for the detection of *Escherichia coli* O157:H7. RSC Adv 5:45092–45097

CAS Article Google Scholar

34. Li DJ, Feng YY, Zhou L, Ye ZZ, Wang JP, Ying YB, Ruan CM, Wang RH, Li YB (2011) Label-free capacitive immunosensor based on quartz crystal Au electrode for rapid and sensitive detection of *Escherichia coli* O157:H7. Anal Chim Acta 687:89–96

CAS Article Google Scholar

35. Shen ZQ, Hou NN, Jin M, Qiu ZG, Wang JF, Zhang B, Wang XW, Wang J, Zhou DS, Li JW (2014) A novel enzyme-linked immunosorbent assay for detection of *Escherichia coli* O157:H7 using immunomagnetic and beacon gold nanoparticles. Gut Pathog 6:14–21

Article Google Scholar

Download references

Acknowledgements

This work was supported by the National Natural Science Foundation of China (NSFC) (Grant No.: 81471747), the National Natural Science Foundation of China (NSFC) (Grant No.: 81601570), Zhejiang Provincial Natural Science Foundation of China (Grant No.: LQ16C190002).